energies

MDPI

Article

Electronic Properties of Typical Molecules and the Discharge Mechanism of Vegetable and Mineral Insulating Oils

Yachao Wang, Feipeng Wang *, Jian Li *, Suning Liang and Jinghan Zhou

State Key Laboratory of Power Transmission Equipment & System Security and New Technology, School of Electrical Engineering, Chongqing University, Chongqing 400044, China; wangyachao@cqu.edu.cn (Y.W.); 20141101004@cqu.edu.cn (S.L.); lxr1236@126.com (J.Z.)

* Correspondence: fpwang@cqu.edu.cn (F.W.); lijian@cqu.edu.cn (J.L.); Tel.: +86-023-65102434 (F.W.); +86-023-6510-2437 (J.L.)

Received: 25 January 2018; Accepted: 24 February 2018; Published: 28 February 2018

Abstract: Vegetable insulating oil may replace the mineral insulating oil used in large power transformers due to its extraordinary biodegradability and fire resistance. According to component analysis, 1-methylnaphthalene and eicosane are considered the typical molecules in mineral oil. Triolein and tristearin are considered the typical molecules in vegetable oil. The ionization potential (IP) and the variation of highest occupied molecular orbital (HOMO) of typical molecules under an external electric field are calculated using quantum chemistry methods. The calculation results show that the IP of the triolein molecule is comparable to that of the 1-methylnaphthalene molecule. The mechanisms of losing electrons are discussed, based on the analysis of HOMO composition. The insulation characteristics of the triolein and tristearin are more likely to be degraded under an external electric field than those of 1-methylnaphthalene and eicosane. Due to the fact that the number density of low IP molecules groups in vegetable oil is much greater than that in mineral oil, the polarity effect in vegetable oil is more obvious than that in mineral oil. This eventually leads to different streamer characteristics in vegetable oil and mineral oil under positive polarity and negative polarity.

Keywords: vegetable oil; mineral oil; electronic property; streamer; space charge; density functional theory

1. Introduction

Vegetable insulating oil is a nontoxic, reproducible and environmental dielectric fluid [1–7]. It can be used as a substitute for mineral insulating oil, in transformer and oil-filled cables [8–11]. The basic physical, chemical and electrical properties of vegetable oil and mineral oil are listed in Table 1 [3]. It is attracting increasing research interest due to its high fire point of above 300 °C [4], which significantly improves the safety level of the power grid. Moreover, the 21-day degradation rate of vegetable oil is up to 97% by the CEC-L-33 test (Coordinating European Council, Leicester), which is superior to mineral oil with 30% [5]. Generally speaking, insulating materials are very sensitive to moisture, such as insulation paper and low-density polyethylene [12,13]. The frequency breakdown voltage of mineral oil will collapse when the moisture is up to 30 ppm, however, the frequency breakdown voltage of vegetable oil will not obviously decrease when the moisture is up to 320 ppm [6,14]. Vegetable oil absorbs the moisture in insulation paper, leading to much more prolonged lifetime of oil-paper insulations [7].

Table 1. Basic physical, chemical and electrical properties of vegetable oils and a mineral oil [3].

Parameter	Camellia Oil	FR3 Oil	Mineral Oil
Appearance	**Light Yellow**	**Light Green**	**Transparent**
Density (20 °C)/kg·m^{-3}	0.90	0.92	<0.895
Viscosity (40 °C)/mm^2·s^{-1}	39.9	34.1	≤13.0
Pour point/°C	−28	−21	<−22
Flash point/°C	322	316	≥135
Acid value/mgKOH·g^{-1}	0.03	0.04	≤0.03
Interfacial tension/mN·m	25	24	≥40
AC breakdown voltage/kV	70	56	≥35
Dissipation factor(90 °C)/%	0.88	0.89	≤0.1
Volume resistivity/Ω·m	1×10^{10}/90 °C	2×10^{11}/25 °C	7×10^{11}/25 °C
Relative permittivity	2.9/90 °C	3.2/25 °C	2.2/90 °C

Vegetable oil has shown comparable electrical properties to mineral oil by some standard tests [8]. However, comparing with mineral oil, fast streamer seems to appear easily in vegetable oil especially when the oil gap is longer than 50 mm. Liu's study shows that [15], under positive polarity, the streamer velocity in vegetable oil is about 10 km/s at 50 mm of oil gap and reaches 30 km/s at 100 mm. The streamer velocity in mineral oil remains at a constant of 1–2 km/s for oil gaps of 25–100 mm under positive polarity. However, under negative polarity, the streamer velocity in vegetable oil seems to be suppressed and the streamer velocity in mineral oil obviously increases with the increasing oil gap. For example, the streamer velocity in mineral oil is about 6 km/s at 75 mm of oil gap under negative polarity, even higher than that in vegetable oil. The fast streamer (>10 km/s) in the insulating liquid may connect the electrodes, resulting in serious disaster. However, the streamer propagation is affected by many factors such as air-pressure, temperature, impurities and moisture. The mechanisms of streamer propagation are not completely understood.

To date, considerable results have focused on the assessment of differences and similarities between vegetable oil and mineral oil based on experimental measurements and analysis. There is a lack of investigation at the molecular level into explaining the electrical discharge phenomena happening in the oils. Density functional theory (DFT) is a quantum chemistry method to calculate the electronic structure. DFT is widely used to speculate about the properties of molecular and condensed matter in both physics and chemistry [16,17]. The molecular components of insulating oils are very plentiful and we chose several typical molecules to study the molecular characteristics associated with electric discharge.

Mineral oil, as transformer oil, is from petroleum by distillation at a temperature of 260–400 °C. According to the component analysis, mineral oil is dominated by hydrocarbons that include the aromatic, paraffinic and naphthenic [18–20]. Aromatic usually has two benzene rings (e.g., 1-methylnaphthalene molecule) and the total proportion of aromatic is about 5%. Paraffinic and naphthenic usually have 16~22 carbon units (e.g., eicosane molecule) and the total proportion of paraffinic and naphthenic is about 95%. For vegetable oil, the component analysis has indicated that the main molecules are triglycerides [21–25]. The triglyceride molecule can be considered a glycerol molecule esterified by three fatty acid molecules. The fatty acids usually have 14~22 carbon units. The unsaturated fatty acids (e.g., oleic acid, generating triolein molecule in vegetable oil) hold the majority among the fatty acids (about 90%). A small amount of saturated fatty acids (e.g., stearic acid, generating tristearin molecule in vegetable oil) are included as well (about 10%).

In this work, according to the component analysis, 1-methylnaphthalene and eicosane are considered the typical molecules in mineral oil. Triolein and tristearin are considered the typical molecules in vegetable oil. The electronic properties of typical molecules are calculated using the quantum chemistry method. The mechanisms of fast and slow streamers in vegetable oil and mineral oil are discussed based on the calculations.

2. Methods

According to the component analysis, the four typical molecules are considered including 1-methylnaphthalene, eicosane, triolein and tristearin. The models for the typical molecules with a Cartesian axis are shown in Figure 1.

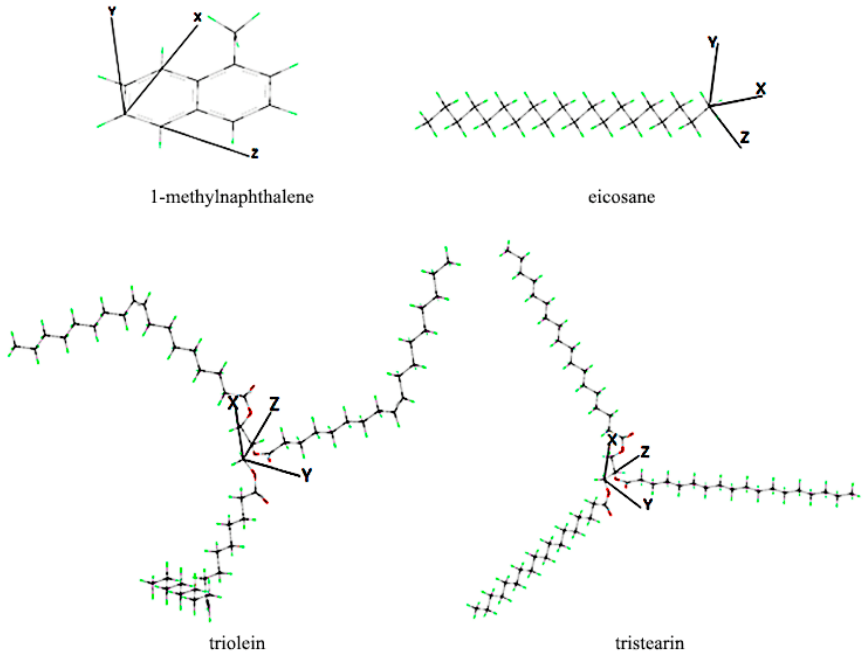

Figure 1. Models of typical molecules with Cartesian axis. Gray: C, red: O, green: H.

The IPs of the typical molecules are calculated by quantum chemistry methods based on density functional theory. The calculations are carried out using the Gaussian 09 program package [26]. The B3LYP method is employed at 6-31G* basis set [27,28].

The geometries of the molecules are optimized for energy minimization. The energy of a positive ion is calculated based on the geometry optimized. The *IP* of molecule A is defined as the energy difference of neutral molecule A and corresponding positive ion A^+, written as:

$$IP = E^{A^+} - E^A \tag{1}$$

The polarizable continuum model (PCM) is used to calculate the *IP* [29]. In PCM, the surrounding liquid for a given molecule is considered as a continuum dielectric with a dielectric constant ε. It is set to be 3.0 for vegetable oil and 2.2 for mineral oil. The DFT method (B3LYP) at the 6-31G* basis set is used as before. The definition of the *IP* in liquid phase can be defined as:

$$IP = E^{A^+} - E^A + V_0, \tag{2}$$

where V_0 is the energy of a quasi-free electron in a condensed state. The values of V_0 are generally much less than the *IP* of the molecules (<0.1 eV). Hence, the V_0 is neglected in this work [30].

The electronic properties of molecules will be changed under the external field, resulting in changes of the ionization characteristic [31,32]. The electric field intensity of streamer initiation is about 10^8 V/m [33–35]. However, the electric field intensity of streamer fast propagation is at least 10^9 V/m [19]. The external field directions include X, X-, Y, Y-, Z and Z-. Electronic properties of a triolein molecule under an external electric field were investigated in our previous study and the direction of the electric field is along the Z axis [31].

Koopman's theorem points out that there is a negative correlation between the IP and the energy of the highest occupied molecular orbital (HOMO). The increase of HOMO energy means that the electrons easily escape from the molecular orbital and the insulation capacity declines. The HOMO energies of those molecules under an external field are calculated. Under an external electric field, the Hamiltonian of the molecule system is the sum of molecule Hamiltonian and interaction Hamiltonian, described as [36]:

$$H = H_0 + H_{\text{int}} \tag{3}$$

The H_{int} is the interaction Hamiltonian between the electric field and molecule, which can be described as:

$$H_{\text{int}} = -\boldsymbol{\mu}\cdot\boldsymbol{F} \tag{4}$$

where $\boldsymbol{\mu}$ is dipole moment and $\boldsymbol{F}$ is radiation field. External electric fields are applied along the X, X-, Y, Y-, Z and Z-axis. The intensities are 0.0005 a.u. and 0.005 a.u. 1 a.u. of electric field is equal to 5.14×10^{11} V/m. The intensities are namely 2.57×10^{8} V/m and 2.57×10^{9} V/m.

3. Results and Discussion

3.1. Wavenumber of Functional Group

The infrared spectrum reflects the molecular structure. However, the molecular structure determines the physicochemical and biological properties of the molecule. Wavenumbers of functional groups of the molecules are calculated. A scale factor of 0.96 for B3LYP/6-31G* is used to address the fundamental error [37]. The results are listed in Table 2 together with the experimental data published previously [38–40]. The spectral peak of a wavenumber calculated for 1-methylnaphthalene molecule is 3072.9 cm^{-1} from C–H stretching on benzene ring. The spectral peak of a wavenumber calculated for eicosane molecule is 3072.9 cm^{-1} from C–H stretching. For a triolein molecule, the wavenumbers of C=O stretching are 1775.7 cm^{-1}, 1778.2 cm^{-1} and 1784.9 cm^{-1} from the three C=O double bonds; the wavenumbers of C=C stretching are 1673.4 cm^{-1}, 1673.5 cm^{-1} and 1673.6 cm^{-1} from the three C=C double bonds. For a tristearin molecule, the wavenumbers of C=O stretching are 1775.6 cm^{-1}, 1778.2 cm^{-1} and 1784.8 cm^{-1} from the three C=O double bonds. The experimental values of wavenumbers are also listed in this table, which show consistencies with theoretical results.

Table 2. Wavenumber of functional groups.

Typical Molecule	Vibration Mode	Wavenumber (cm^{-1})	
		Calculated Value	Experimental Value
1-Methylnaphthalene	C–H stretching	3072.9	3077 [1]
Eicosane	C–H stretching	2954.9	2934 [1]
Triolein	C=O stretching	1775.7, 1778.2, 1784.9	1746 [2], 1745 [3]
	C=C stretching	1673.4, 1673.5, 1673.6	1653 [2], 1654 [3]
Tristearin	C=O stretching	1775.6, 1778.2, 1784.8	

[1,2,3] Experimental values are taken from [38–40], respectively.

3.2. Ionization Potentials and HOMO

The IPs of the typical molecules are calculated by the methods mentioned in Section 2 and the results are listed in Table 3. As shown in the table, the liquid-phase calculations are smaller than the gas-phase values. This is ascribed to the fact that the energy of a neutral molecule E^A is almost unchanged and the energy of a positive ion E^{A+} is decreased in PCM. The IP of a triolein molecule in liquid phase is 6.65 eV, which is comparable to that of a 1-methylnaphthalene molecule. The IP of a tristearin molecule in liquid phase is 7.73 eV, which is near to that of eicosane molecule. The calculated

value of 1-methylnaphthalene is close to the experimental value, which assures the reliability of our method.

Table 3. Ionization potentials of typical molecules.

Typical Molecule	IP in Gas Phase (eV)	IP in Liquid Phase (eV)
1-Methylnaphthalene	7.51	6.25/6.20 [1]
Eicosane	8.78	7.92
Triolein	7.24	6.65
Tristearin	8.21	7.73

[1] The experimental value in Ref [41].

Electrons move on the HOMO of a molecule and may escape from the orbital by way of the energy obtained from collision, illumination or otherwise [33,42]. Collisions occur between neutral molecules and free electrons accelerated in the high electric field. A neutral molecule is ionized during the collision. A neutral molecule can also be ionized under illumination, namely photo-ionization. Table 4 shows the HOMO energies of typical molecules. The HOMO energies of typical molecules in the gas phase are −5.67 eV, −7.61 eV, −6.28 eV and −7.32 eV, respectively. The liquid-phase results are almost equal to the gas-phase ones. As discussed in Section 2, in PCM, the surrounding liquid of the molecule is considered as a continuum dielectric with a dielectric constant ε. The PCM does not much affect the electron structure of a neutral molecule.

Table 4. Highest occupied molecular orbital (HOMO) energies of typical molecules.

Typical Molecule	HOMO in Gas Phase (eV)	HOMO in Liquid Phase (eV)
1-Methylnaphthalene	−5.67	−5.71
Eicosane	−7.61	−7.60
Triolein	−6.28	−6.33
Tristearin	−7.32	−7.46

The isosurface of the HOMO of a 1-methylnaphthalene molecule is shown in Figure 2. The HOMO compositions are analyzed by the Mulliken method using the Multiwfn program [43]. C10, C11, C5 and C2 make the primary contribution to the HOMO with the percentage of 18.33%, 17.23%, 15.12% and 14.99%, respectively. Furthermore, the contribution of each C atom consists of two P-shells (10.87% and 7.41%, take C10 for example). It can be speculated that the electrons of these atoms may escape from the HOMO of 1-methylnaphthalene. The contributions of all the H atoms are all less than 1.5%. The H atoms are least likely to provide electronic in the discharge process.

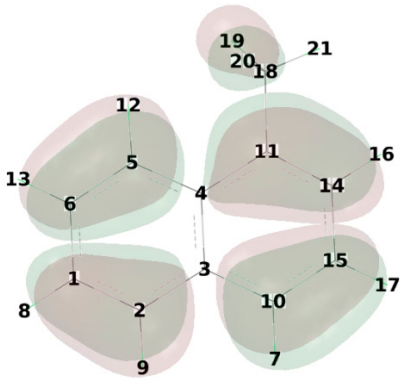

Figure 2. Isosurface of HOMO of 1-methylnaphthalene molecule.

The isosurface of the HOMO of an eicosane molecule is shown in Figure 3 and only H's labels are excluded in order to be concise. HOMO compositions are distributed across all the C atoms. In the order of the most contribution, it goes: C29 with 8.15%, C32 with 8.15%, C26 with 7.88%, C35 with 7.87%, C23 with 7.35%, C38 with 7.36%, C20 with 6.61%, C41 with 6.61%, C17 with 5.71%, C44 with 5.71%, C14 with 4.70%, C47 with 4.70%, C11 with 3.63%, C50 with 3.64%, C8 with 2.70%, C53 with 2.70%, C5 with 1.73%, C56 with 1.73%, C1 with 1.05% and C57 with 1.05%, respectively. From the results listed above, the C atoms in the molecule center are more likely to lose the electrons than the C atoms in two-ends.

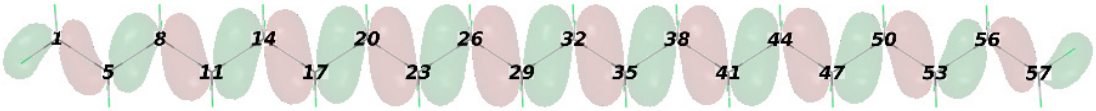

Figure 3. Isosurface of HOMO of eicosane molecule.

Figure 4 shows the isosurface of the HOMO of a triolein molecule. HOMO compositions are contributed by the C atoms in the *cis* C=C functional group at the position Sn-2. C100 and C102 make the primary contribution to the HOMO with the percentage of 39.67% and 39.66%, respectively. The contributions from the two C atoms consist of two P-shells (about 22.46% and 16.92% for C100; 22.45% and 16.92% for C102). The *cis* C=C functional group makes the triolein molecule very active. The molecule is easily ionized under a high electrical field. The IP of a triolein molecule is comparable to that of a 1-methylnaphthalene molecule.

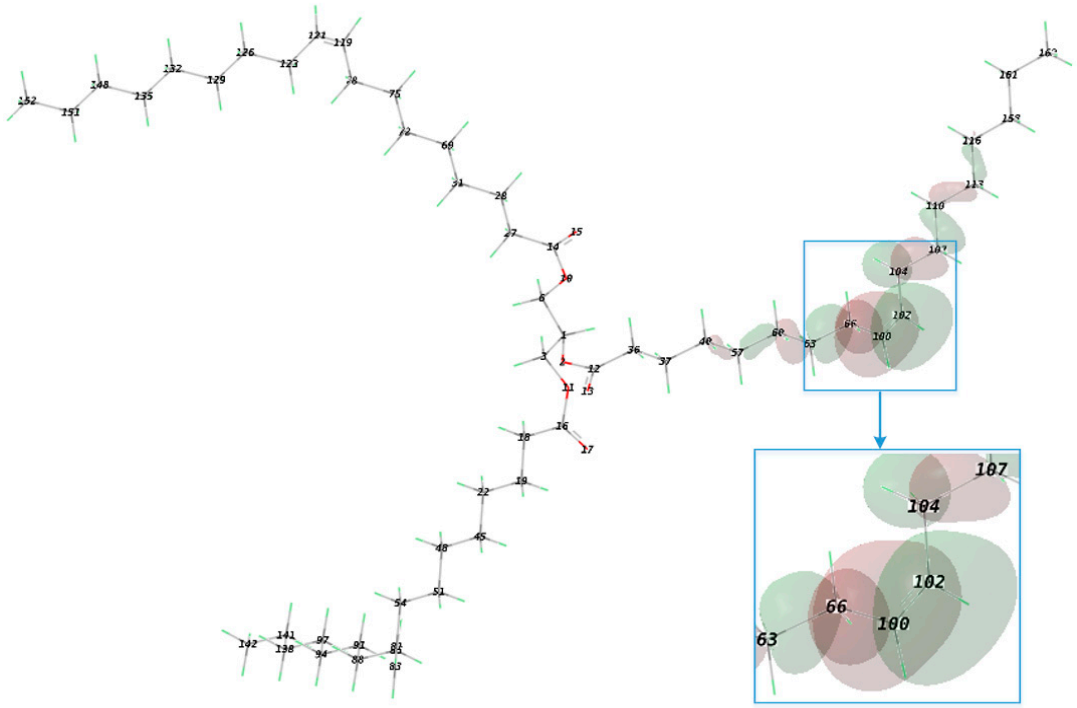

Figure 4. Isosurface of HOMO of triolein molecule.

The isosurface of the HOMO of a tristearin molecule is shown in Figure 5. O17 and the neighboring atom C18 make the primary contribution with a percentage of 68.42% and 10.62%, respectively. The contribution of O17 consists of two P-shells (about 43.60% and 24.83%). Compared with the *cis* C=C, the C=O has improved chemical stability. The IP of a tristearin molecule is comparable to that of an eicosane molecule.

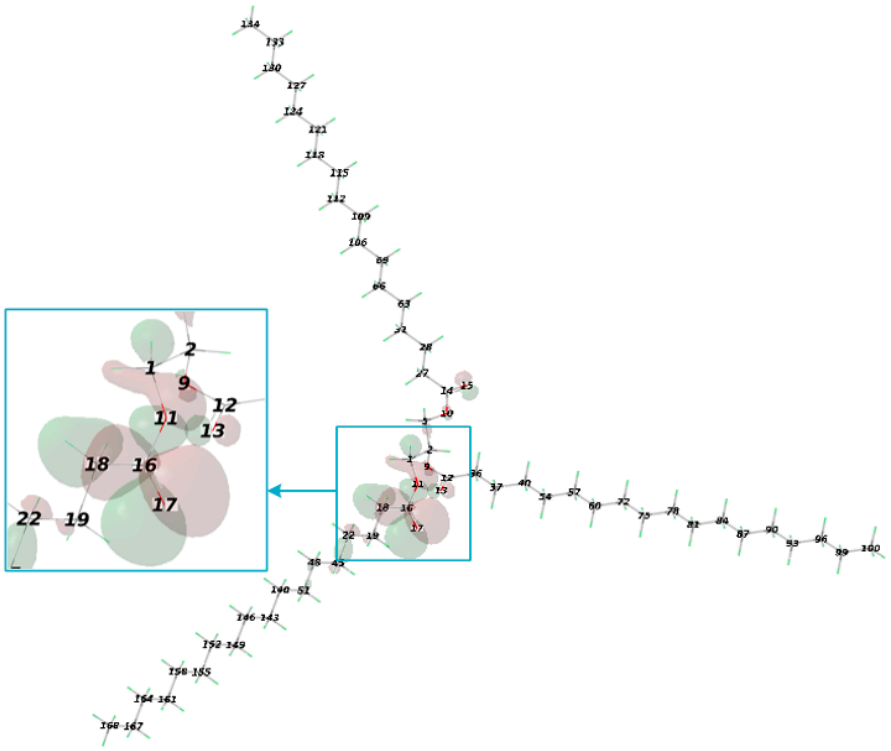

Figure 5. Isosurface of HOMO of tristearin molecule.

3.3. HOMO Variation under External Electric Field

The electronic structure of a molecule is not invariable under an external electric field as discussed in Section 2. The HOMO energy variations of the four typical molecules with applied fields are shown in Figure 6. The electric field intensities are 2.57×10^8 V/m and 2.57×10^9 V/m. The external field directions include X, X-, Y, Y-, Z and Z- of the Cartesian axis as shown in Figure 1. The HOMO energies of the four molecules have slight variations in all directions when the electric field intensity is 2.57×10^8 V/m, as shown in Figure 6. When the electric field intensity is 2.57×10^9 V/m, the HOMO energies change obviously. It is noticed that the HOMO energies of the two triglyceride molecules, including the triolein molecule and the tristearin molecule, increase sharply in all directions. There is a negative correlation between the IP and the energy of the HOMO. That means that the insulation characteristics of triolein and tristearin are more likely to be degraded under an external electric field than those of 1-methylnaphthalene and eicosane.

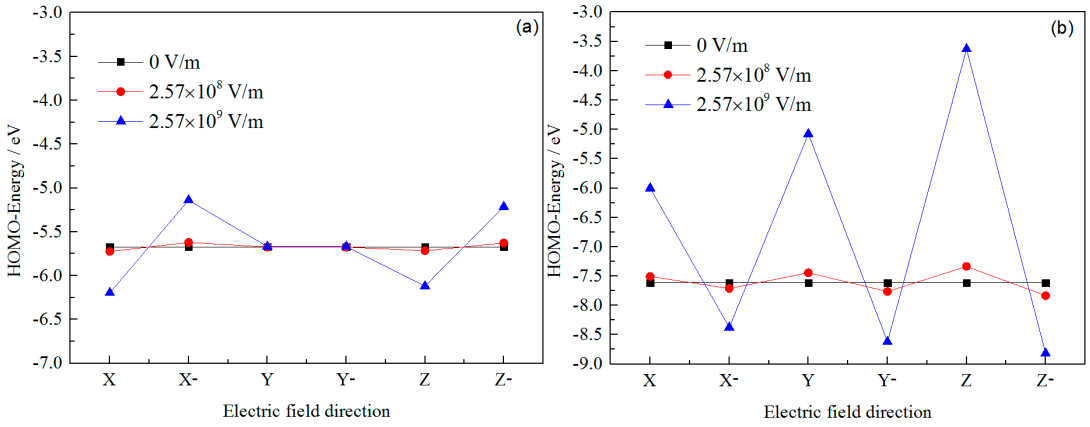

Figure 6. *Cont.*

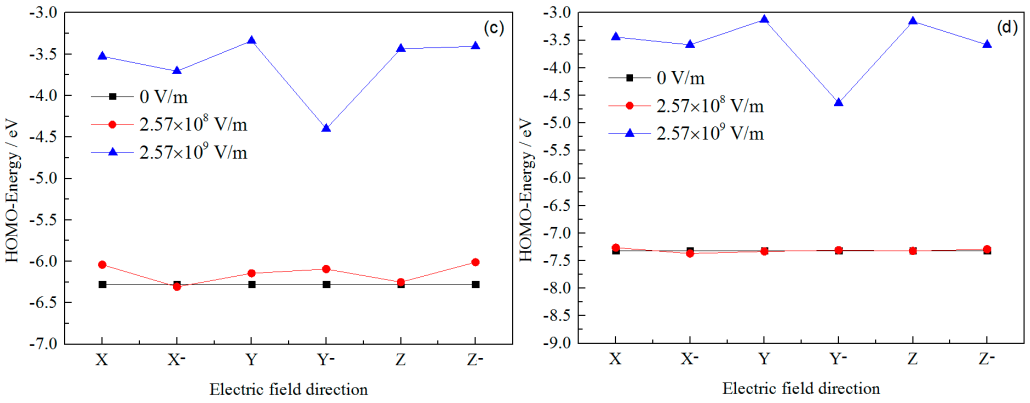

Figure 6. HOMO energy variations with applied fields: (**a**) 1-Methylnaphthalene; (**b**) eicosane; (**c**) triolein; and (**d**) tristearin.

Performance degradation of insulating material is affected by many factors, such as impurity, moisture or ageing [44,45]. Under the external electric fields, the variations of HOMO energy can be ascribed to the variations of composition of the HOMO. Figure 7 shows the isosurface of HOMO of molecule under the external electric field along X-axis with the intensity of 2.57×10^9 V/m. For 1-Methylnaphthalene as shown in Figure 7a, C10, C11, C5 and C2 also make the primary contribution to the HOMO, which are similar with the molecule under no external electric field as shown in Figure 2. However, the contribution rates of C5 and C2 increased to 16.81% and 16.77%, respectively. For triolein, as shown in Figure 7c, C81 and C83 make the primary contribution to the HOMO with the percentage of 40.12% and 34.04%, respectively. Comparison of Figures 4 and 7c, it is noticed that the total contribution rate of atoms of *cis* C=C decreases and the contribution rate of the atoms in the end of the carbon chain increases under the external electric field.

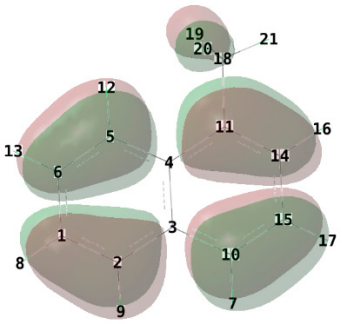

(**a**)

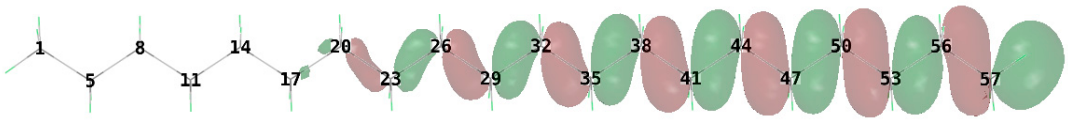

(**b**)

Figure 7. *Cont.*

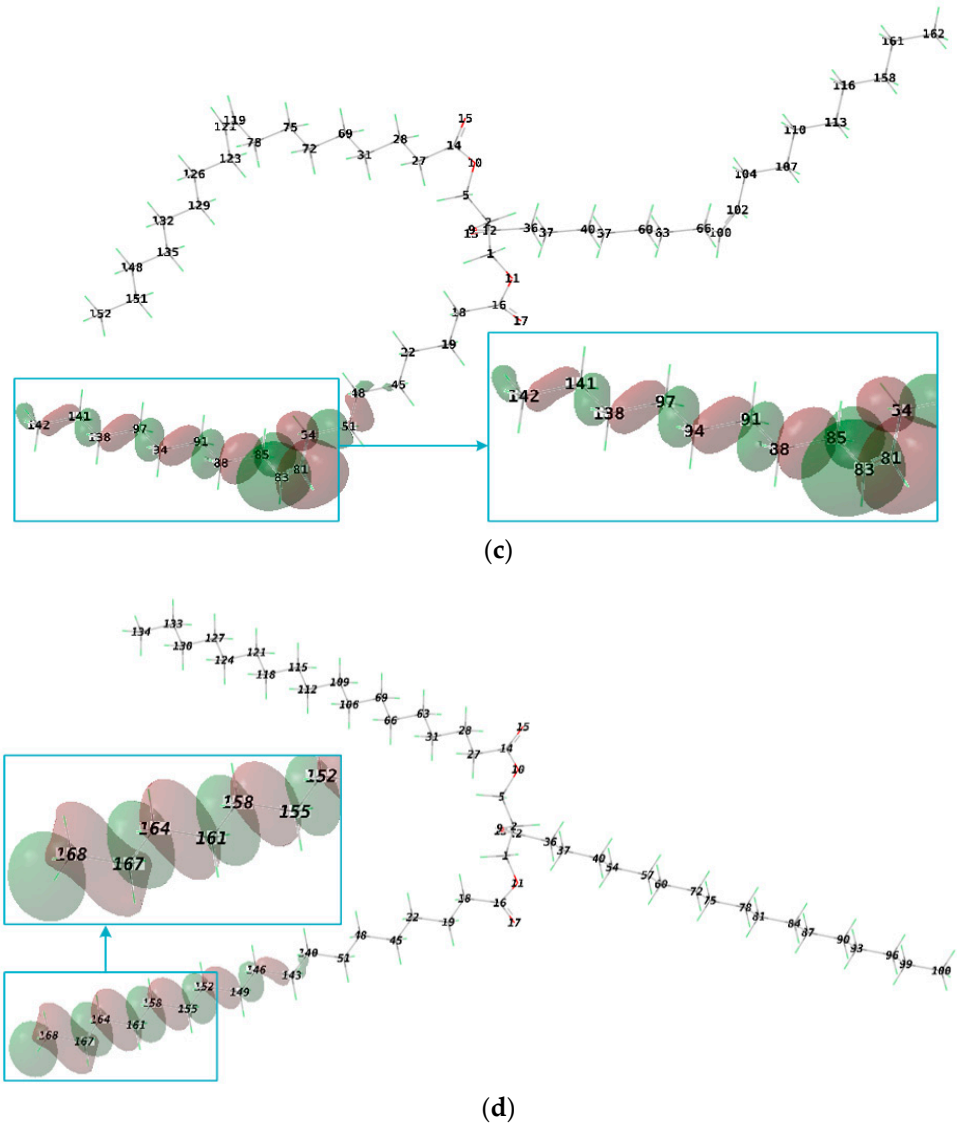

Figure 7. Isosurface of HOMO of molecule under the external electric field along X-axis with the intensity of 2.57×10^9 V/m: (**a**) 1-methylnaphthalene; (**b**) eicosane; (**c**) triolein; and (**d**) tristearin.

4. Discharge Mechanisms

4.1. Streamer Characteristic Effected by the Distribution of Ionization Potential

Each oil is considered in terms of a low IP molecules group and a high IP molecules group. The corresponding number densities within each group are N_L and N_H, respectively. For vegetable oil, the low IP molecules group is formed by triolein molecules and the high IP molecules group is composed of tristearin molecules. It is found that $N_L >> N_H$ in vegetable oil. For mineral oil, the low IP molecules group is represented by 1-methylnaphthalene molecules and the high IP molecules group contains eicosane molecules. It is recognized that $N_L << N_H$ in mineral oil. Additionally, the IP of the low IP molecules group in vegetable oil is comparable to the IP of the low IP molecules group in mineral oil.

Consider the positive streamer in oils. When enough voltage is applied to the needle electrode, remarkable ionization of molecules happens. The generated electrons rush to the positive electrode quickly due to the high electron mobility and the positive ions are left to form the tip of the streamer. The generated positive ions move to the negative electrode slowly due to the low ion mobility.

The separation of positive ion and electron will form the induced electric field $\boldsymbol{E}$, which can be written as:

$$\nabla \cdot \boldsymbol{E} = \sum_{\mathrm{i}} e n_{\mathrm{i}} / \varepsilon, \tag{5}$$

where n_{i} is the number density of the molecule i which has been ionized and ε is the dielectric constant. Assume that all the low IP molecules are ionized when breakdown happens. Equation (5) can be revised as:

$$\nabla \cdot \boldsymbol{E} = e N_{\mathrm{L}} / \varepsilon. \tag{6}$$

Due to $N_{\mathrm{L}} >> N_{\mathrm{H}}$ in vegetable oil, there will be sufficient low IP molecules being ionized that form the powerful induced electric field $\boldsymbol{E}$, which facilitates the further ionization of molecules. The streamer velocities of vegetable oils can reach or exceed 10 km/s. Due to $N_{\mathrm{L}} << N_{\mathrm{H}}$ in mineral oil, the limited low IP molecules can be ionized to form the weak induced electric field $\boldsymbol{E}$. The streamer velocities of mineral oil remain quite slow as 1–2 km/s. In order to observe the fast streamer in mineral oil, a higher voltage is needed after breakdown happens. Assume that all the high IP molecules are ionized when a fast streamer appears in mineral oil. Sufficient high IP molecules can be ionized to form a powerful induced electric field $\boldsymbol{E}$. Equation (5) can be revised as:

$$\nabla \cdot \boldsymbol{E} = e(N_{\mathrm{L}} + N_{\mathrm{H}}) / \varepsilon. \tag{7}$$

4.2. Polarity Effect and Space Charge

In Reference [15], the breakdown voltage of vegetable oil is lower than that of mineral oil both under positive polarity and under negative polarity. However, it is worth pointing out that the streamer velocity of vegetable oil can reach 10~30 km/s (fast streamer) under positive polarity but be severely suppressed under negative polarity. The streamer velocity of mineral oil is even higher than that of vegetable oil under negative polarity. It is almost impossible that the streamer velocity of mineral oil is higher than that of vegetable oil under positive polarity. Probably because the number density of low IP molecules group in vegetable oil is much greater than that in mineral oil, that is $N_{\mathrm{LV}} >> N_{\mathrm{LM}}$, the breakdown voltage of vegetable oil is always lower than that of mineral oil.

Also, due to $N_{\mathrm{LV}} >> N_{\mathrm{LM}}$, the polarity effect in vegetable oil is more obvious than that in mineral oil. This eventually leads to the different streamer characteristics in vegetable oil and mineral oil under positive polarity and negative polarity. Figure 8 shows the polarity effect in vegetable oil and mineral oil.

Under positive polarity in Figure 8a, the electrons enter the positive needle electrode after the neutral molecules are ionized. The positive ions are left near the needle tip. The space charges weaken the field near the tip and strengthen the field forward. The effects of space charges on the electric field in vegetable oil are more significant than that in mineral oil. The strengthened field facilitates the further ionization process. The induced electric field will dominate the streamer propagation in the long oil gaps. The insulation degradation of molecules in such high fields will further facilitate the streamer propagation. Hence, the fast streamer appears easily in vegetable oils.

Under negative polarity in Figure 8b, the electrons rush to the positive plane electrode after the neutral molecules are ionized. The positive ions are left behind. The space charges strengthen the field near the tip and weaken the field forward. The effects of space charges on field in vegetable oil are also more significant than that in mineral oil. The weakened field represses the further ionization process. Hence, the streamer velocities of mineral oil even surpass those of vegetable oil in long oil gaps.

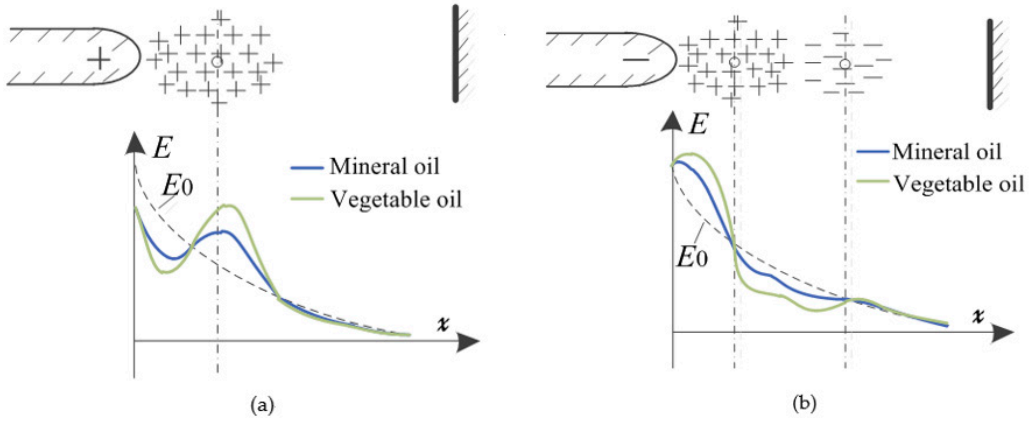

Figure 8. Polarity effect in vegetable oil and mineral oil: (**a**) positive polarity; and (**b**) negative polarity.

5. Conclusions

In this work, 1-methylnaphthalene and eicosane are selected as the typical molecules in mineral oil. Triolein and tristearin are selected as the typical molecules in vegetable oil. The electronic properties of the typical molecules are calculated using the quantum chemistry method (B3LYP/6-31G*) based on density functional theory. The mechanisms of fast and slow streamers in mineral oil and vegetable oil are discussed based on the calculations. Several conclusions are summarized as follows:

(1). The IP of a triolein molecule is comparable to that of a 1-methylnaphthalene molecule. The IP of a tristearin molecule is comparable to that of an eicosane molecule, especially in the liquid phase. The mechanisms of losing electrons are discussed based on the analysis of HOMO composition.

(2). The HOMO energy variations with applied fields are calculated. The insulation characteristics of triolein and tristearin are more likely to be degraded under an external electric field than those of the 1-methylnaphthalene and eicosane.

(3). Due to the fact that the number density of the low IP molecules group in vegetable oil is much greater than that in mineral oil, the polarity effect in vegetable oil is more obvious than that in mineral oil. This eventually leads to different streamer characteristics in vegetable oil and mineral oil under positive polarity and negative polarity.

Acknowledgments: The work is supported by the National Natural Science Foundation of China (No. 51425702). The authors appreciate the National "111" Project of the Ministry of Education of China (No. B08036) and the State Key Program of National Natural Science Foundation of China (No. U1537211). The computational resources and Gaussian program are provided by National Supercomputing Center in Shenzhen (Gaussian 09 D01: TCP-Linda). We also thank to Special Program for Applied Research on Super Computation of the NSFC-Guangdong Joint Fund (the second phase).

Author Contributions: Feipeng Wang and Jian Li structured this work. Yachao Wang and Jinghan Zhou conducted the molecule simulation. Yachao Wang and Suning Liang analyzed the data and wrote the paper, Feipeng Wang and Jian Li revised the manuscript.

Conflicts of Interest: The authors declare no conflict of interest.

References

1. Jing, Y.; Timoshkin, V.; Given, M.J.; Macgregor, S.G.; Wilson, M.P.; Wang, T. Dielectric properties of natural ester, synthetic ester Midel 7131 and mineral oil Diala D. In Proceedings of the Power Modulator and High Voltage Conference, San Diego, CA, USA, 3–7 June 2012; pp. 63–66.
2. Fernández, I.; Delgado, F.; Ortiz, F.; Ortiz, A.; Fernández, C.; Renedo, C.J.; Santisteban, A. Thermal degradation assessment of Kraft paper in power transformers insulated with natural esters. *Appl. Therm. Eng.* **2016**, *104*, 129–138. [CrossRef]
3. Xiang, C.; Zhou, Q.; Li, J.; Huang, Q.; Song, H.; Zhang, Z. Comparison of dissolved gases in mineral and vegetable insulating oils under typical electrical and thermal faults. *Energies* **2016**, *9*, 312. [CrossRef]

4. Lashbrook, M.; Gyore, A.; Martin, R. A review of the fundamental dielectric characteristics of ester-based dielectric liquids. *Proc. Eng.* **2017**, *202*, 121–129. [CrossRef]
5. Oommen, T.V.; Claiborne, C.C.; Mullen, J.T. Biodegradable electrical insulation fluids. In Proceedings of the Electrical Insulation Conference and Electrical Manufacturing and Coil Winding Conference, Rosemont, IL, USA, 25–25 September 1997; pp. 465–468.
6. Zou, P.; Li, J.; Sun, C.; Liao, R.; Zhang, Z. Influences of moisture content on insulation properties of vegetable insulating oil. *High Vol. Eng.* **2017**, *37*, 1627–1633.
7. Liao, R.; Hao, J.; Chen, G.; Ma, Z.; Yang, L. A comparative study of physicochemical, dielectric and thermal properties of pressboard insulation impregnated with natural ester and mineral oil. *IEEE Trans. Dielectr. Electr. Insul.* **2011**, *18*, 1626–1637. [CrossRef]
8. Cargill. Envirotemp FR3 Fluid. Available online: https://www.cargill.com/bioindustrial/envirotemp/fr3 (accessed on 1 November 2017).
9. Kolcunová, I.; Kurimský, J.; Cimbala, R.; Petráš, J.; Dolník, B.; Džmura, J.; Balogh, J. Contribution to static electrification of mineral oils and natural esters. *J. Electrost.* **2017**, *88*, 60–64. [CrossRef]
10. Pourrahimi, A.M.; Olsson, R.T.; Hedenqvist, M.S. The role of interfaces in polyethylene/metal-oxide nanocomposites for ultrahigh-voltage insulating materials. *Adv. Mater.* **2018**, *30*, 1703624. [CrossRef] [PubMed]
11. Aljurea, M.; Becerraa, M.; Pallon, L.K.H. Electrical conduction currents of a mineral oil-based nanofluid in needle-plane configuration. In Proceedings of the IEEE Conference on Electrical Insulation and Dielectric Phenomena, Toronto, ON, Canada, 16–19 October 2016; pp. 687–690.
12. Nilsson, F.; Karlsson, M.; Pallon, L.; Giacinti, M.; Olsson, R.T.; Venturi, D.; Gedde, U.W.; Hedenqvist, M.S. Influence of water uptake on the electrical DC-conductivity of insulating LDPE/MgO nanocomposites. *Compos. Sci. Technol.* **2017**, *152*, 11–19. [CrossRef]
13. Pourrahimi, A.M.; Pallon, L.K.H.; Liu, D.; Hoang, T.A.; Gubanski, S.; Hedenqvist, M.S.; Olsson, R.T.; Gedde, U.W. Polyethylene nanocomposites for the next generation of ultralow transmission-loss HVDC cables: Insulation containing moistureresistant MgO nanoparticles. *ACS Appl. Mater. Interfaces* **2016**, *8*, 14824–14835. [CrossRef] [PubMed]
14. Fofana, I.; Borsi, H.; Gockenbach, E. Fundamental investigations on some transformer liquids under various outdoor conditions. *IEEE Electr. Insul. Mag.* **2001**, *8*, 1040–1047. [CrossRef]
15. Liu, Q.; Wang, Z.D. Streamer characteristic and breakdown in synthetic and natural ester transformer liquids under standard lightning impulse voltage. *IEEE Trans. Dielectr. Electr. Insul.* **2011**, *18*, 285–294. [CrossRef]
16. Kohn, W. Nobel Lecture: Electronic structure of matter—Wave functions and density functionals. *Rev. Mod. Phys.* **1999**, *71*, 1253–1266. [CrossRef]
17. Kumar, J.; Nemade, H.B. Adsorption of small molecules on niobiumdoped graphene: A study based on Density Functional Theory. *IEEE Electron Device Lett.* **2018**, *39*, 296–299. [CrossRef]
18. Wedin, P. Electrical breakdown in dielectric liquids-a short overview. *IEEE Electr. Insul. Mag.* **2014**, *30*, 20–25. [CrossRef]
19. Rozga, P. Streamer propagation in small gaps of synthetic ester and mineral oil under lightning impulse. *IEEE Trans. Dielectr. Electr. Insul.* **2015**, *22*, 2754–2762. [CrossRef]
20. Claiborne, C.C.; Pearce, H.A. Transformer fluids. *IEEE Electr. Insul. Mag.* **1989**, *5*, 16–19. [CrossRef]
21. Wang, X.; Zeng, Q.; Verardo, V.; Contreras, M.d.M. Fatty acid and sterol composition of tea seed oils: Their comparison by the "FancyTiles" approach. *Food Chem.* **2017**, *233*, 302–310. [CrossRef] [PubMed]
22. Fatemi, S.H.; Hammond, E.G. Glyceride structure variation in soybean varieties. I. Stereospecific analysis. *Lipids* **1977**, *12*, 1032–1036. [CrossRef]
23. Lísa, M.; Holčapek, M. Triacylglycerols profiling in plant oils important in food industry, dietetics and cosmetics using high-performance liquid chromatography–atmospheric pressure chemical ionization mass spectrometry. *J. Chromatogr. A* **2008**, *1198–1199*, 115–130. [CrossRef] [PubMed]
24. Takagi, T. Stereospecific analysis of triacyl-sn-glycerols by chiral high-performance liquid chromatography. *Lipids* **1991**, *26*, 542–547. [CrossRef]
25. Zeb, A. Triacylglycerols composition, oxidation and oxidation compounds in camellia oil using liquid chromatography–mass spectrometry. *Chem. Phys. Lipids* **2012**, *165*, 608–614. [CrossRef] [PubMed]
26. Frisch, M.J.; Trucks, G.W.; Schlegel, H.B.; Scuseria, G.E.; Robb, M.A.; Cheeseman, J.R.; Scalmani, G.; Barone, V.; Mennucci, B.; Petersson, G.A.; et al. *Gaussian 09*; Gaussian Inc.: Wallingford, CT, USA, 2013.

27. Becke, A.D. Density—Functional thermochemistry. III. The role of exact exchange. *J. Chem. Phys.* **1993**, *98*, 5648–5652. [CrossRef]
28. Lee, C.; Yang, W.; Parr, R.G. Development of the Colle-Salvetti correlation-energy formula into a functional of the electron density. *Phys. Rev. B* **1988**, *37*, 785–789. [CrossRef]
29. Cossi, M.; Scalmani, G.; Rega, N.; Barone, V. New developments in the polarizable continuum model for quantum mechanical and classical calculations on molecules in solution. *J. Chem. Phys.* **2002**, *117*, 43–54. [CrossRef]
30. Ingebrigtsen, S.; Smalo, H.S.; Astrand, P.O.; Lundgaard, L.E. Effects of electron-attaching and electron-releasing additives on streamers in liquid cyclohexane. *IEEE Trans. Dielectr. Electr. Insul.* **2009**, *16*, 1524–1535. [CrossRef]
31. Wang, Y.; Wang, F.; Li, J.; Huang, Z.; Liang, S.; Zhou, J. Molecular structure and electronic properties of triolein molecule under an external electric field related to streamer initiation and propagation. *Energies* **2017**, *10*, 510. [CrossRef]
32. Xu, G.L.; Xie, H.X.; Yuan, W.; Zhang, X.Z.; Liu, Y.F. Properties of a Si_2N molecule under an external electric field. *Chin. Phys. B* **2012**, *21*, 053101. [CrossRef]
33. Tobazcon, R. Prebreakdown phenomena in dielectric liquids. *IEEE Trans. Dielectr. Electr. Insul.* **1994**, *1*, 1132–1147. [CrossRef]
34. Beroual, A.; Zahn, M.; Badent, A.; Kist, K.; Schwabe, A.J.; Yamashita, H.; Yamazawa, K.; Danikas, M.; Chadband, W.D.; Torshin, Y. Propagation and structure of streamers in liquid dielectrics. *IEEE Electr. Insul. Mag.* **1998**, *14*, 6–17. [CrossRef]
35. Badent, R.; Hemmer, M.; Konekamp, U.; Julliard, Y.; Schwab, A.J. Streamer inception field strengths in rape-seed oils. In Proceedings of the Annual Report Conference on Electrical Insulation and Dielectric Phenomena, Victoria, BC, Canada, 15–18 October 2000; pp. 272–275.
36. Buckingham, A.D. Direct method of measuring molecular quadrupole moments. *J. Chem. Phys.* **1959**, *30*, 1580–1585. [CrossRef]
37. The National Institute of Standards and Technology (NIST). Computational Chemistry Comparison and Benchmark Data Base. Available online: http://cccbdb.nist.gov/vibscalejust.asp (accessed on 31 October 2016).
38. The National Institute of Standards and Technology (NIST). NIST Chemistry Webbook. Available online: http://webbook.nist.gov/cgi/cbook.cgi?ID=C90120&Units=SI&Type=IR-SPEC&Index=2#IR-SPEC (accessed on 1 December 2017).
39. Christy, A.A.; Xu, Z.F.; Harrington, P.D.B. Thermal degradation and isomerisation kinetics of triolein studied by infrared spectrometry and GC–MS combined with chemometrics. Chem. Phys. *Lipids* **2009**, *158*, 22–31. [CrossRef] [PubMed]
40. Kos, A.; Tefelski, D.B.; Kosciesza, R.; Rośtocki, A.J.; Roszkiewicz, A.; Ejchart, W.; Jastrzebski, C.; Siegoczyńsk, R.M. Certain physico-chemical properties of triolein and methyl alcohol–triolein mixture under pressure. *High Press. Res.* **2007**, *27*, 39–42. [CrossRef]
41. Holroyd, R.A.; Preses, J.M.; Boettcher, E.H.; Schmidt, W.F. Photoconductivity induced by single-photon excitation of aromatic molecules in liquid hydrocarbons. *Chem. Inf.* **1984**, *15*, 744–749. [CrossRef]
42. Sparks, M.; Mills, D.L.; Warren, R.; Holstein, T.; Maradudin, A.A.; Sham, L.J.; Loh, J.E.; King, D.F. Theory of electron-avalanche in solids. *Phys. Rev. B* **1981**, *24*, 3519–3536. [CrossRef]
43. Lu, T.; Chen, F.W. *Multiwfn 3.3.8*; Kein Research Center for Natural Sciences: Beijing, China, 2016.
44. Akhlaghi, S.; Pourrahimi, A.M.; Hedenqvist, M.S.; Sjöstedt, C.; Bellander, M.; Gedde, U.W. Degradation of carbon-black-filled acrylonitrile butadiene rubber in alternative fuels: Transesterified and hydrotreated vegetable oils. *Polym. Degrad. Stab.* **2016**, *123*, 69–79. [CrossRef]
45. Akhlaghi, S.; Pourrahimi, A.M.; Sjöstedt, C.; Bellander, M.; Hedenqvist, M.S.; Gedde, U.W. Degradation of fluoroelastomers in rapeseed biodiesel at different oxygen concentrations. *Polym. Degrad. Stab.* **2017**, *136*, 10–19. [CrossRef]